Supplemental Information: Measurement of Oxygen Concentrations in Bacterial Biofilms using Transient State Monitoring by Single Plane Illumination Microscopy

A. Karampatzakis, J. Sankaran, K. Kandaswamy, S. A. Rice, Y. Cohen and T. Wohland*

*twohland@nus.edu.sg

References and links

1. T. Sandén, G. Persson, P. Thyberg, H. Blom and J. Widengren "Monitoring kinetics of highly environment sensitive states of fluorescent molecules by modulated excitation and time-averaged fluorescence intensity recording," Anal. Chem. **79**, 3330–41.
2. M. Geissbuehler, T. Spielmann, A. Formey, I. Marki, M. Leutenegger, B. Hinz, K. Johnsson, D. van de Ville and T. Lasser "Triplet imaging of oxygen consumption during the contraction of a single smooth muscle cell (A7r5)," Biophysical Journal **98**, 339–349 (2010).
3. A. Deshpande and N. Iyer "Correlation of fluorescence and lasing properties in Eosin Y," J. of Luminescence. **46**, 339–344 (1990).
4. T. Spielmann, H. Blom, M. Geissbuehler, T. Lasser and J. Widengren "Transient state monitoring by total internal reflection fluorescence microscopy," J. Phys. Chem. B. **114**, 4035–46 (2010).
5. J. Mücksch, T. Spielmann, E. Sisamakis and J. Widengren "Transient state imaging of live cells using single plane illumination and arbitrary duty cycle excitation pulse trains," J. Biophotonics **8**(5), 392–400 (2014).
6. S. Reindl and A. Penzkofer "Triplet quantum yield determination by picosecond laser double–pulse fluorescence excitation," Chem. Phys. **213**, 429–38 (1996).
7. A. Penzkofer, A. Beidoun and M. Daiber "Intersystem-crossing and excited-state absorption in Eosin Y solutions determined by picosecond double pulse transient absorption measurements," J. Lumin. **51**, 297–314 (1992).
8. A. Penzkofer and A. Beidoun "Triplet–triplet absorption of Eosin Y in methanol determined by nanosecond excimer laser excitation and picosecond light continuum probing," Chemical Physics **177**(1), 203–216 (1993).
9. J. R. Lakowicz "Principles of Fluorescence Spectroscopy," 3rd Edition, Springer ISBN: 978-0-387-31278-1 (2006).
10. L. W. Lo, C. J. Koch and D. F. Wilson "Calibration of oxygen–dependent quenching of the phosphorescence of Pd-meso-tetra (4-carboxyphenyl) porphine: a phosphor with general application for measuring oxygen concentration in biological systems," Anal. Biochem. **236**, 153–60 (1996).
11. Y. Zhang, C. K. Ng, Y. Cohen and B. Cao "Cell growth and protein expression of Shewanella oneidensis in biofilms and hydrogel-entrapped cultures," Molecular BioSystems **10**, 1035–1042 (2014).
12. S. L Chua, S. Y–Y. Tan, M. T. Rybtke, Y. Chen. S. A. Rice, S. Kjelleberg, T. Tolker–Nielsen, L. Yang and M. Givskova "Bis–(3=–5=)–Cyclic Dimeric GMP Regulates Antimicrobial Peptide Resistance in Pseudomonas aeruginosa," Antimicrobial Agents and Chemotherapy. **57**(5), 2066–2075 (2013).
13. T. Spielmann, L. Xu, A. K. B. Gad, S. Johansson and J. Widengren "Transient state microscopy probes patterns of altered oxygen consumption in cancer cells," The FEBS Journal **281**(5), 1317–32 (2014).
14. R. Nilsson, P. Merkel and D. Kearns "Kinetic properties of the triplet states of methylene blue and other photosensitizing dyes," Photochemistry and photobiology. **16**(2):109-116 (1972).
15. J. M. Vanderkooi, G. Maniara, T. J. Green, D. F. Wilson "An optical method for measurement of dioxygen concentration based upon quenching of phosphorescence," J. Biol Chem **262**(12), 5476–82 (1987).

S.1. Mathematical formulation

The system of equations that describes a three–level energy system is:

$$\frac{d}{dt}\begin{bmatrix} P_0 \\ P_1 \\ P_T \end{bmatrix} = \begin{bmatrix} \frac{P_1}{\tau_{10}} + \frac{P_T}{\tau_T} - \frac{P_0}{\tau_{01}} \\ -\frac{P_1}{\tau_{10}} - \frac{P_1}{\tau_{isc}} + \frac{P_0}{\tau_{01}} \\ \frac{P_1}{\tau_{isc}} - \frac{P_T}{\tau_T} \end{bmatrix} \tag{S1}$$

where P_0, P_1 and P_T are the populations of S_0, S_1 and S_T respectively, τ_{10} is the lifetime for the singlet state relaxation, τ_{isc} is the intersystem crossing lifetime from the excited singlet state to the triplet state, τ_{01} is the excitation lifetime, and τ_T is the triplet state lifetime. The complete solution of the above system is a second order differential equation involving the four transition rates [1, 2].

The time–averaged fluorescence emission intensity of a fluorophore illuminated by an isodose of light, when delivered by a train of rectangular pulses, can be described by the equations below [2]:

$$I(\vec{r}) = \gamma(\vec{r})\left(1 - \frac{\tau_T P_T^{eq}\left(1 - exp\left(-\frac{T-w}{\tau_T}\right)\right)}{1 - exp\left(-\frac{T-w}{\tau_T} + k_2 w\right)} \times \frac{exp(k_2 w) - 1}{w}\right) \tag{S2}$$

where w denotes the pulse width, T the period of the pulse train, and τ_{01}, τ_{10}, and τ_T are the lifetimes for the three transitions, as defined earlier. Additionally, k_2 describes the population rate of the triplet state after onset of excitation, P_T^{eq} is the relative triplet state population at equilibrium for constant excitation, and $\gamma(\vec{r})$ is a scaling factor that depends on the concentration of fluorophores and the detection efficiency, defined as:

$$k_2 = -\left(\frac{\tau_{01} + \tau_{10} + q_T \tau_T}{\tau_T(\tau_{01} + \tau_{10})}\right) \tag{S3}$$

$$P_T^{eq} = \frac{q_T \tau_T}{\tau_{01} + \tau_{10} + q_T \tau_T} \tag{S4}$$

$$\gamma(\vec{r}) = \eta \Gamma(\vec{r}) \frac{q_f}{\tau_{01} + \tau_{10} + q_T \tau_T} \tag{S5}$$

where

$$q_f = \frac{\tau_{isc}}{\tau_{isc} + \tau_{10}} \tag{S6}$$

is the quantum efficiency of the fluorophores, and

$$q_T = \tau_{10}/\tau_{isc} \tag{S7}$$

is the triplet quantum yield, $\Gamma(\vec{r})$ is the concentration of fluorophores and η is a conversion factor between the emitted intensity and the digital readout of the camera.

As seen in Equation (S2), the time–averaged fluorescence intensity in a TRAST monitoring experiment depends on all the four transition rates. The excitation time, τ_{01}, is limited by the illumination intensity and the absorption cross–section of the molecule. The excitation rate for a particular dye and experimental settings, is therefore considered constant and can be calculated by:

$$k_{01}^{-1} = \tau_{01} = \frac{hc}{\lambda P_{\text{laser}} \sigma(\lambda)} \tag{S8}$$

where h is the Planck constant, c the speed of light, λ the excitation wavelength, P_{laser} the excitation power and $\sigma(\lambda)$ the molecular absorption cross–section. Using Equation (S8) and for laser powers that match our experimental setup, τ_{01} for Eosin Y is calcuated in range of a few ns, which is in agreement to the experimentally measured value of 1.55 ns [3].

The triplet relaxation rate and intersystem crossing are more difficult to measure and depend on environmental factors such as the oxygen content and the viscosity of the solvent. The triplet relaxation time for Eosin Y has been found to change from approximately 2 to 30 µs between a completely aerated and deaerated solution, respectively [4, 5]. Likewise, a range for intersystem crossing times can be found in the literature (from approximately 2 ns to 5 ns [4–7]. It should be noted that both the measured triplet relaxation and intersystem crossing times depend, additionally, on the experimental method used to determine them.

S.2. Derivation of calibration model for faster measurements

Figure S1a shows the TRAST curves, modelled for various triplet relaxation times. The selected range of triplet relaxation times cover the cases of oxygen–depleted to air–saturated samples, in room temperature.

The maximum contrast within each curve can be seen between the intensities recorded with the shortest and longest pulse widths. Therefore, we define the relative decrease as $(I_{short} - I_{CW})/I_{short}$ where I_{short} is the intensity recorded from a train of pulses of low duty cycle (typically 1%) which allow relaxation of molecules to the ground state, and I_{CW} the intensity recorded when continuously illuminating the sample for the same amount of time (duty cycle = 100%).

A solution to predict this relative decrease is derived from equation S2 and plotted on Figure S1b against increasing triplet relaxation times. Relative decreases of 64.7% and 94.7% were calculated when the triplet relaxation time was increased from 2 µs to 20 µs, respectively. The values of I_{CW} can be calculated analytically by setting $w = T$ which gives:

$$I|_{w=T}(\tau_T) = H\frac{A}{B + C\tau_T} \tag{S9}$$

where H is a constant factor depending on the concentration of the fluorophores and acquisition efficiency, and,

$$\begin{aligned} A &= \tau_{isc} \\ B &= \tau_{isc}(\tau_{ex}\tau_{isc} + \tau_{10}\tau_{isc} + \tau_{ex}\tau_{10} + \tau_{10}^2) \\ C &= \tau_{10}^2 + \tau_{10}\tau_{isc}. \end{aligned} \tag{S10}$$

On the other hand, I_{short} needs to be solved numerically for the relative difference between the two to be calculated.

Additionally, the triplet time can be expressed as a function of the quencher concentration –in our case, oxygen– by re–writing the Stern–Volmer equation as:

$$\tau_T = \frac{\tau_{T0}}{1 + k_q\tau_{T0}[O_2]} \tag{S11}$$

where τ_{T0} is the triplet lifetime in the absence of the quencher and k_q is a quenching constant obtained by the Smoluchowski equation $k_q = 4\pi RDN/1000$, where R is the collision radius (the sum of the molecular radii of the fluorophore and quencher), D is the sum of the diffusion coefficients of the fluorophore and quencher, N is Avogadro's number and 1/1000 is a normalisation factor to convert molarity to molecules/cm [9].

By combining equations (S9 – S11) we can calculate the relative decrease in fluorescence for different values of oxygen. When transition rates characteristic of Eosin Y are considered, a

linear relationship can be seen to hold ($R^2 = 0.99$) for oxygen concentration values ranging from deaerated to air–saturated solutions (Figure S2).

S.3. Sample preparation

S.3.1. Bulk solutions

Eosin Y (Sigma–Aldrich, Singapore) stock samples of mM concentration were prepared in ethanol (Sigma Chemicals, St. Louis, U.S.A.). The samples were further diluted in double-distilled water (ddH2O) to final concentration of 2 μM. In the full TRAST monitoring experiments, bulk solution was placed in heat–sealed sample bags made from thin transparent foil with a refractive index matching that of water (Katco Ltd., United Kingdom). Each of the bags contained approximately 50 μL of the solution. Viscosity of the solution was controlled by addition of sucrose, where applicable.

The oxygen content in a solution can be controlled by titrating L–Ascorbic Acid (AA), in a reaction catalysed by Ascorbate Oxidase (AO) [2, 10], according to:

$$\text{L-Ascorbic Acid} + O_2 \longrightarrow 2\,H_2O + 2\,\text{Dehydroascorbate} \tag{S12}$$

AA was purchased from Sigma–Aldrich and dissolved 65 μM. AO from *Cucurbita sp.* (lyophilised powder purchased from Sigma–Aldrich) was reconstituted in 20 mM sodium phosphate (NaH_2PO_4) buffer. The enzyme has an activity of 1,000 to 3,000 units per mg protein. One unit will oxidize 1.0 μM of AA to dehydroascorbate per min at pH 5.6 at 25^oC.

In order to acquire the calibration curve the sample needs to be accessible to the probe. For that matter, larger bags that can hold approximately 800 μL were created (Figure S3a). The bags were left open at the top to allow for parallel measurements (Figure S4). Three units of AO were added prior to placement of the sample in the microscope and aliquots of AA were injected and gently mixed inside the bag by pipetting, before the onset of acquisition. Measurements were taken during the course of atmospheric oxygen uptake, while the absolute values were monitored by the probe. Measurements were repeated by replenishing the solution.

S.3.2. Hydrogel beads

Calcium alginate hydrogels were prepared using the methods described in [11]. Alginate acid (Acros Organics, U.K.) solutions (3% wt/vol) in water were prepared and autoclaved. Filter–sterilised $CaCl_2$ (100 mM) solution was poured in a 6 well plate (Nunclon Flat, Thermoscientific) in columns approximately 2 mm tall. Drops of 10 – 20 μL of alginate acid were dropped into the well using a pipette. The cross linking was almost instantaneous. The drops were left to settle for approximately 20 min before they were washed twice with sterile water and kept in sterile water for storage, if necessary. The alginate hydrogels beads were transferred to heat–sealed bags made from thin transparent foil with a refractive index matching that of water (Katco Ltd., United Kingdom) that included the bulk dye solution (Figure S3b).

S.3.3. Bacterial biofilms

Pseudomonas aeruginosa (PAO1) were grown overnight in LB Broth (Difco) 40 g/L in a shaking incubator at 37^oC, 200 rpm. The culture was diluted to an OD600 ≈ 2.0 and 300 μL were injected into a fluorinated ethylene propylene (FEP) tubing near the entry port of the flow cell. The inoculum remained in the flow cell to settle for 1 h without flow, at room temperature. The flow of the minimal medium (ABT supplemented with 5 g/L of glucose plus 2 g/L of Casamino Acid (ABTGC) [12] was then resumed at a rate of ≈ 6 ml/h. A 6–Roller peristaltic pump (Langer Instruments, U.S.A.) was used to supply the flow. The flow cell system with FEP tubing of 30 mm long, 2.1 mm ID and 2.3 mm OD and was used in all experiments. The FEP tubings were

autoclaved and flushed with 10% (v/v) bleach, then thoroughly rinsed in sterile milli–Q and then primed with ABTGC medium before the start of every experiment.

Prior to imaging, one of the four sides of the square FEP tube on which biofilms had grown was carefully cut out using a surgical scalpel and placed in the thin foil FEP heat–sealing bag which contained approximately 50 μL of the dye (Eosin Y, 2 μM, shown on Figure S3. The bag was placed in the microscope chamber at a slight angle (Figure S4) allowing cross sections of the colonies to be imaged.

S.3.4. Microscopic setup

A 488 nm laser (OBIS LX, Coherent Inc., Santa Clara, CA, USA) is used and its beam is expanded about 5 times by two sets of achromatic lenses. It then passes through an achromatic cylindrical lens (f = 75 mm, Edmund optics, Singapore). The resulting beam over–illuminates the back focal aperture of the low NA illumination objective (SLMPlan 20X / 0.25, Olympus, Singapore) to obtain a light sheet $\approx$ 1.2 μm thick. The illumination objective has a working distance of WD = 21 mm. This provides the necessary space to bring the light sheet into the focal plane of the detection objective (LUMPLFLN 60x/1.0 W, WD = 2.0 mm, Olympus, Singapore). The sample mounting unit consists of a custom built sample chamber (Physics mechanical workshop, NUS, Singapore) and motorized linear x–, y– and z–stages together with a rotation stage (XYZ–linear stages: 3×8MT184–13DC and rotation stage: 8MR174–1–20, Standa Ltd., Lithuania). The detection objective was mounted on a piezo flexure objective scanner (P–721 PIFOC, Physik Instruments, Singapore) to control the objective in nm precision. A fluorescence emission filter (BrightLine HC525/50, Semrock Inc., New York) was mounted behind the detection objective, before a standard tube lens (part no. LU074700, f = 180 mm, Olympus, Singapore) used to image the sample onto the camera. An Andor iXon X3 860 EMCCD (Andor Technology, Belfast, UK) camera was used in the experiments.

Modulation of the laser output is digitally controlled using a custom–build program on LabView (National Instruments, Austin, TX) that can create finite–length pulse trains of desired characteristics. The pulse sequence is fed from the computer to both the laser and the camera via a terminal box (NI CB–68LPR, National Instruments, Austin, TX) connected to a data acquisition board (NI PCI–6221, National Instruments, Austin, TX). The camera was triggered by the onset of the first pulse and the exposure time was equal to the full length of the pulse train. Pulses of widths as short as 200 ns were validated using a Si switchable gain detector (PDA36A–EC, Thorlabs) connected to an oscilloscope.

Sample	Method [Ref.]	τ_T (µs)	τ_{isc} (ns)
Eosin Y,	Present study	2.16 ± 0.02	1.86 ± 0.02
air–saturated solution	SPIM–TRAST [5]	2.08 ± 0.04	1.34 ± 0.06
	Confocal–TRAST [5]	2.38 ± 0.11	1.32 ± 0.14
	Picosecond double-pulse excitation [6]	-	2.38 ± 0.28
	Flash photolysis [8]	-	1.19 ± 0.11
	TRAST [13]	1.89 ± 0.04	1.18 ± 0.03
Eosin Y,	Present study	16.52 ± 0.06	3.03 ± 0.01
deaerated solution	TRAST [13]	29.41 ± 3.40	2.96 ± 0.25

Table S1. Triplet relaxation and intersystem crossing times for Eosin Y in air–saturated and deaerated solutions, together with values from literature review.

Viscosity (cP)	Slope (Mean ± Standard deviation)
1.00	(−0.96 ± 0.07) E-03
1.30	(−1.06 ± 0.15) E-03
1.80	(−0.77 ± 0.45) E-03
2.90	(−2.17 ± 0.06) E-03
5.50	(−2.25 ± 0.27) E-03
13.5	(−2.25 ± 0.18) E-03

Table S2. Slopes of the linear fit of the relative fluorescence intensity decrease, i.e. $(I_{short} - I_{CW})/I_{short}$, for increasing viscosities by varying sucrose concentrations.

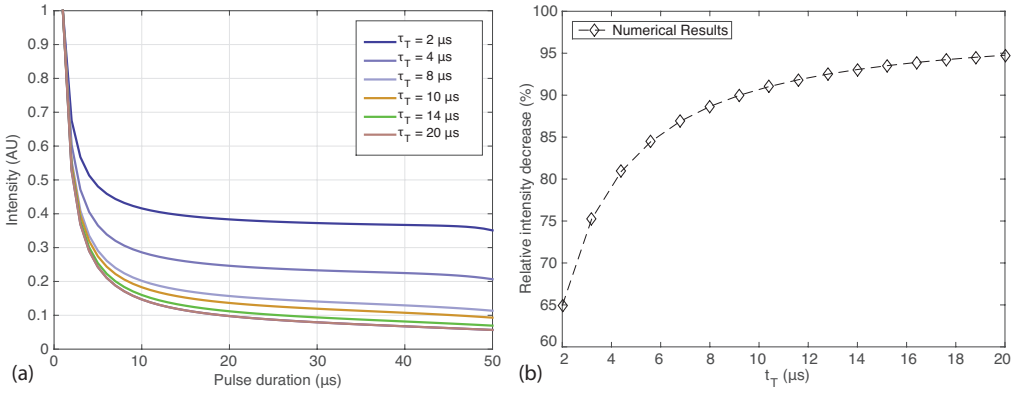

Fig. S1. (a) The effect of different triplet relaxation times on TRAST curves. Parameters used in modelling: $T = 50$ µs, $\tau_{isc} = 2.5$ ns, $\tau_{01} = 2.2$ ns, $\tau_{01} = 3$ ns [5]. (b) Relative decrease in fluorescence, defined as $(I_{short} - I_{CW})/I_{short}$, where I_{short} is the sample fluorescence when illuminated using a low duty cycle (1%), and I_{CW} when using continuous illumination (total illumination time constant), for a range of triplet relaxation times.

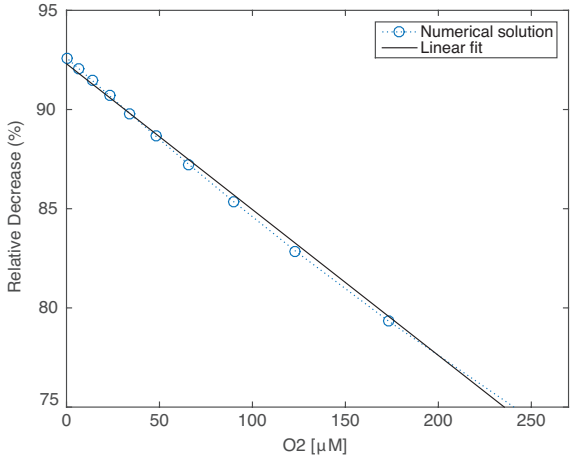

Fig. S2. Relationship between oxygen concentration and relative decrease of fluorescence intensity $(I_{short} - I_{CW})/I_{short}$. Values used for modelling: $k_q = 10^9$ M^{-1} s^{-1} (i.e. Eosin Y in aqueous solution [14]) and $\tau_{T0} = 12$ µs). Linear fit $R^2 = 0.99$. The solution was considered fully aerated at ≈ 250 µM oxygen concentration [15].

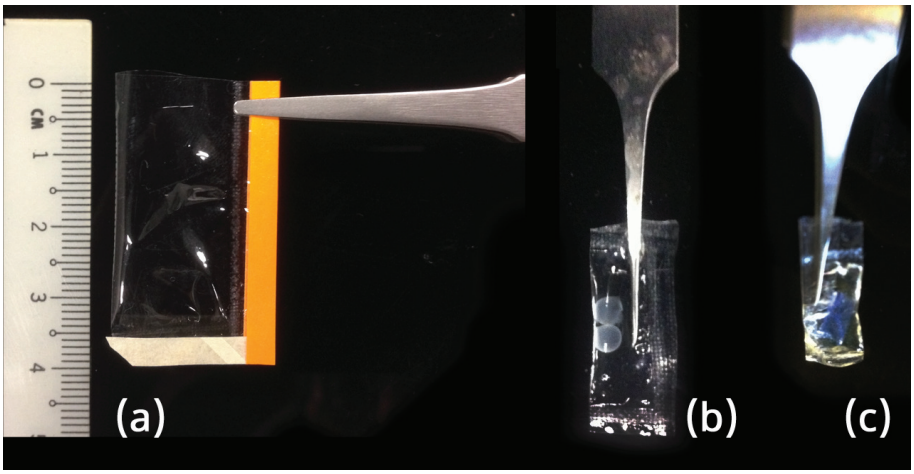

Fig. S3. (a) FEP bag with open top allowing access to the measuring probe in parallel with optical measurements. Used in the calibration experiments. (b) Two alginate acid beads immersed in Eosin Y solution in the thermo–sealed bag. (c) One of the faces of the square tube with biofilm attached, here shown cut out from the tube and placed in the thermo-sealed FEP bag.

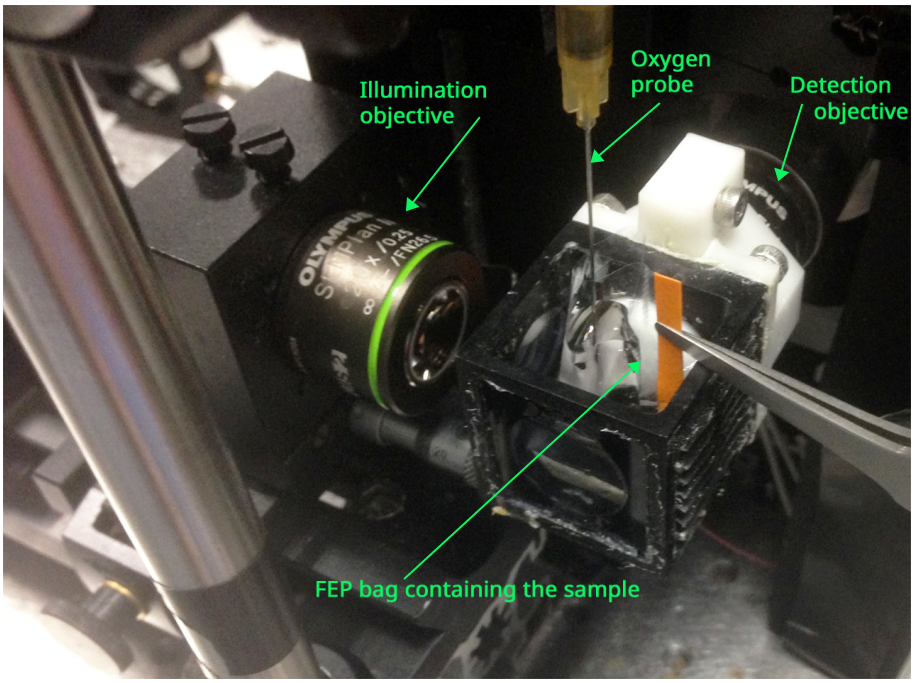

Fig. S4. Experimental setup used during the calibration. The oxygen content of a bag of dye is being measured using an pre–calibrated optical fibre oxygen sensor (FireSting2, Pyro–Science) while at the same time fluorescence intensity is measured using different pulse widths using the SPIM setup.

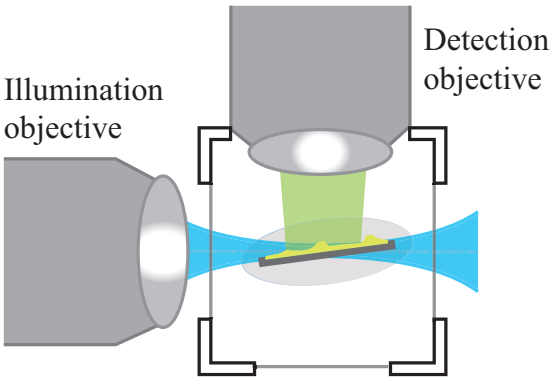

Fig. S5. Illustration of mounting concept for bacterial biofilms in SPIM. One of the surfaces of the square tube which has attached biofilm on, is cut and removed using a scalpel and put in a bag made of thin FEP matching the refractive index of water. The bag is filled with dye solution and placed at a slight angle in respect to the optical axis. Drawing is not to scale.

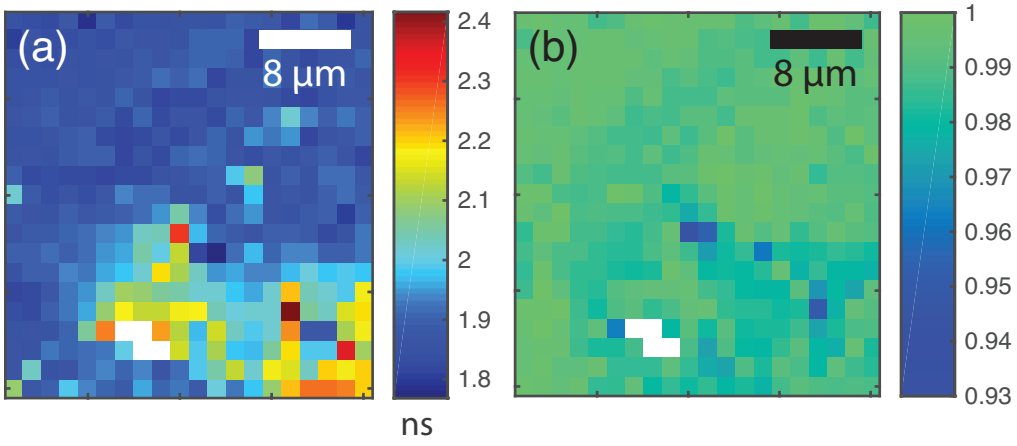

Fig. S6. (a) Extracted intersystem crossing times for a calcium alginate (3% w/w) hydrogel bead, as shown in Figure 5 of main text. (b) R^2 of the fit. The pixel size is 1.6×1.6 µm and white pixels represent areas where the fitting has failed.

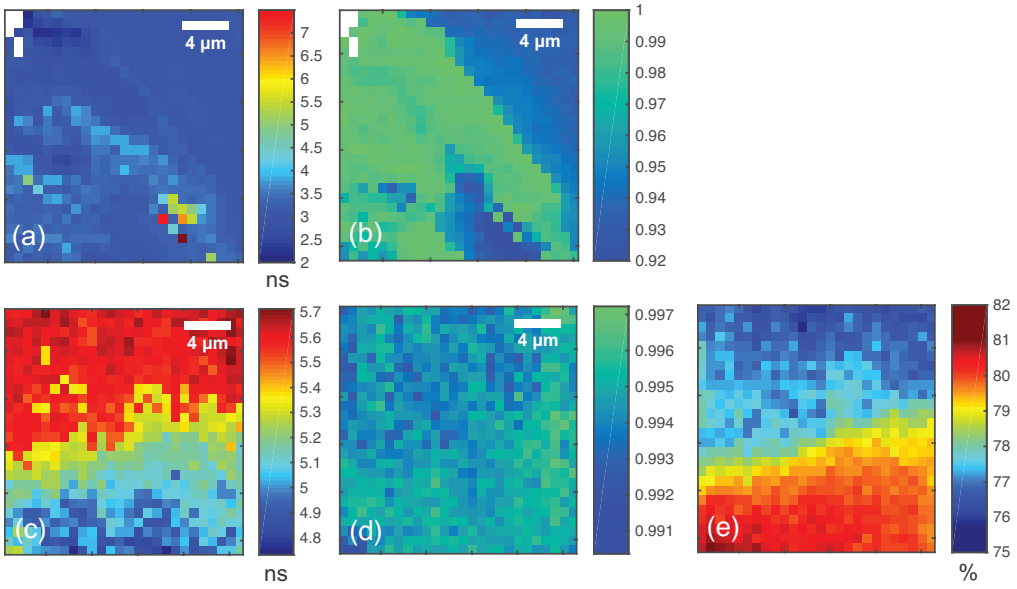

Fig. S7. (a,c) Extracted intersystem crossing times and (b,d) R^2 values of the fit for a *P. aeruginosa* colony, imaged on the fourth day of the biofilm lifecycle in an air–saturated and deaerated solution of Eosin Y, respectively. (e) Relative fluoresence intensity decrease, calculated as $(I_{short} - I_{CW})/I_{short}$ for the colony imaged in deaerated solution. The pixel size is 0.8 ± 0.8 µm and white pixels represent areas where the fitting has failed.